

Long term monitoring of a cable stayed bridge using DuraMote

Marco Torbol*, Sehwan Kim and Masanobu Shinozuka

University of California, Irvine, USA

(Received June 11, 2012, Revised November 25, 2012, Accepted November 30, 2012)

Abstract. DuraMote is a remote sensing system developed for the “NIST TIP project: next generation SCADA for prevention and mitigation of water system infrastructure disaster”. It is designed for supervisory control and data acquisition (SCADA) of ruptures in water pipes. Micro-electro mechanical (MEMS) accelerometers, which record the vibration of the pipe wall, are used detect the ruptures. However, the performance of Duramote cannot be verified directly on a water distribution system because it lacks an acceptable recordable level of ambient vibration. Instead, a long-span cable-stayed bridge is an ideal test-bed to validate the accuracy, the reliability, and the robustness of DuraMote because the bridge has an acceptable level of ambient vibration. The acceleration data recorded on the bridge were used to identify the modal properties of the structure and to verify the performance of DuraMote. During the test period, the bridge was subjected to heavy rain, wind, and a typhoon but the system demonstrates its robustness and durability.

Keywords: remote sensing network; structural health monitoring; system identification; remote monitoring

1. Introduction

The Structural Health Monitoring (SHM) of civil infrastructures has been gaining great interest and new monitoring systems have been introduced to pursue various purposes. For example, Ch developed a remote monitoring system integrated to accelerometers that aggregates data between (2008) data aggregators and sensing nodes through wireless. Kim (2007) developed an optical fiber accelerometer that is free from electromagnetic (EM) interferences and it can therefore be used in environments with strong EM fields. Lynch (2003) developed one of the first prototypes that integrates micro-electro-mechanical-system (MEMS)-type accelerometers with wireless communication capability for civil structures monitoring, which was also developed by Park (2005).

In this paper, the performance of DuraMote system has been validated in terms of the application-driven system flexibility, subject to be confirmed by the deployment on a long-span cable-stayed bridge. The system was originally designed to detect the pipe ruptures in water distribution systems Shinozuka (2010). However, the system can be reconfigured depending on the application requirements. The performances of DuraMote were validated by the field experiment of the Hwamyung Bridge, which is a cable-stayed bridge in South Korea, in terms of high data-fidelity, system flexibility, reliability, robustness, and user friendliness. The additional

*Corresponding author, Ph.D., E-mail: mtorbol@uci.edu

performance criteria such as remote, real-time, and long term monitoring capability were also tested in this experiment. When used for the structural health monitoring of bridges rather than of water distribution systems, some features of DuraMote system has to be modified. The maximum sampling frequency of the system can be reduced and a different set of algorithms for system identification must be used. The modal properties of the bridge were identified using frequency domain decomposition (FDD) Brincker (2001) and they can be compared with the results obtained by Nguyen (2012), which conducted a similar experiment on the same bridge in the same time period. However, rather than FDD they used Subspace Identification (SSI) as system identification algorithm Yi (2004).

The base station is connected to the other components of the system through Wi-Fi and to Internet. Therefore, the base station can be accessed directly on-site, locally through the Wi-Fi network, or remotely through internet. DuraMote sensing system has been developed by concentrating on system flexibility so that it is applicable to other civil infrastructures. The performance of DuraMote when monitoring water distribution systems was verified by laboratory experiment and field deployment Kim (2001) . However, this was the first field test experiment for the structural health monitoring of bridge. Earlier experimental studies on DuraMote are limited to laboratory test, although some field experiments were carried out such as Vincent Thomas Bridge deployment, which was a short term and small scale experiment involving at most 7 sensing nodes. For this reason, key performance characteristics such as accuracy, robustness, flexibility, reliability of the system when used over an extended period of time and in a harsh environment is still largely unknown. Also unexpected software and hardware problems may be emerged due to the long term and the large scale nature of this experiment.

2. The DuraMote system

The proliferation of Micro-Electro-Mechanical Systems (MEMS) technology has facilitated the development of intelligent sensing system for SHM. DuraMote system is also integrated with low noise MEMS-type analogue accelerometers. DuraMote was originally designed for the real-time monitoring and condition assessment of utility water distribution systems particularly during and after natural disasters. In the water distribution system, the sensing nodes are installed at least two joints to identify a damaged link between two adjacent joints with local maximum change in acceleration when pipe ruptures.

The detection method takes advantage of the water hammer effect, which is created by the sudden rupture of the pipe. The water hammer effect is a transient phenomena identified with a difference in pressure Δp that propagates from the point of the rupture to the entire water distribution system. The pressure wave Δp can be detected not only by pressure gauges but also by accelerometers because it generates vibrations in the pipe wall. The wave propagates with a speed c^0 that depends from: the Young modulus, the diameter, and the thickness of the wall of the pipe, Eq. (1)

$$c^0 = \frac{c}{\sqrt{1 + \frac{d}{s} \frac{E}{E_m}}} \quad (1)$$

where c is the speed of sound in water (1410 m/s), d is the diameter of the pipe, s is the thickness of the pipe wall, E/E_m is the ratio between the Young modulus of the pipe and the water Ghetti (1980).

These geometrical and mechanical properties of the water distribution system are known a priori. Therefore, once the nodes of the installed DuraMote system are synchronized it is possible to pinpoint the location of the rupture. The rupture location can be found in near real-time by constructing a contour map of measured acceleration peaks at all nodes. The critical advantage of measuring the acceleration on the pipe surface rather than the pressure at each node stems from the fact that the former requires only contact of the sensor with the water pipe surface whereas the latter needs invasive installment of pressure gauges in the pipe. DuraMote was designed with two components at each node: Gopher, which contains the MEMS accelerometers and it's attached to the surface of the buried pipe, and Roocas, which is the data aggregator unit, it's placed just above ground, and transfers the data to a base station. The details of these and other components and their functions are described in subsections 2.1 and 2.2 below.

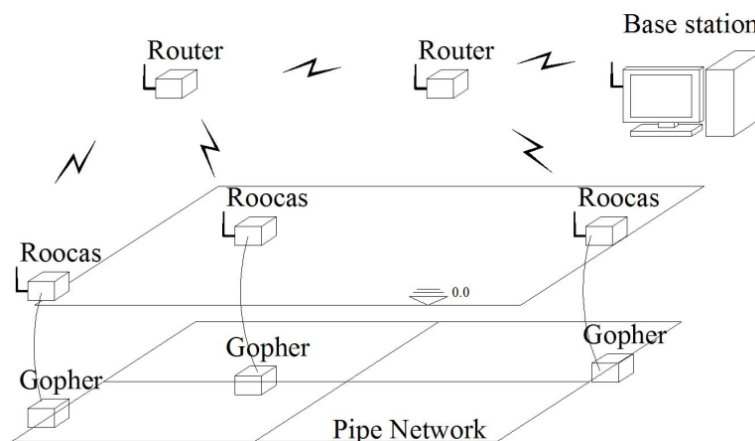


Fig. 1 DuraMote system

2.1 Gopher: Sensing node

Fig. 2 shows a sensing node, Gopher consisting of two stackable printed circuit boards (PCBs). The bottom board is fabricated to extend to multi-channels of accelerometers or integrate different types of sensors for tilt, humidity, gas, temperature etc. Moreover, a programmable signal converter is built on the board, thereby regarding parameters as anti-aliasing filter, cut-off frequency, sampling rate, and post-processing filter can be adjusted by microcontroller unit (MCU). The upper board has MCU and controller area network (CAN) transceiver. It is in charge of collecting the sensing data and transmitting them to a data aggregator through CAN communication line. The CAN supports the bus protocol so that a wireless data aggregator can be daisy-chained connected to multiple Gophers. In fact, DuraMote adopts a power over CAN

(PoCAN) technique. The advantage of PoCAN is that one RJ-9 cable can distribute power from a data aggregator to daisy-chain connected multiple Gophers along with data communication. As a result, it is possible to remove the additional cable for power lines, as well as admit simple and quick installation.

Furthermore, outdoor deployment is needed to consider harsh environment conditions such as severe temperature difference, high humidity, strong wind, and waterproof. Considering the harsh environment condition, DuraMote utilizes NEMA 4+ (i.e., IP66) enclosures to protect our system against heavy rain, high humidity, and high temperature. As mentioned above, Gopher has extension ports to add additional channels depending on deploying places. For the Hwamyung bridge deployment, Gopher placed on the cable had one accelerometer built-in one channel, Gopher placed on the deck had two accelerometers for both vertical and transverse monitoring, and Gopher placed on top of pylon has three accelerometers to monitor longitudinal, transverse and vertical direction.



(a) PCB assembly



(b) Gopher built in a NEMA enclosure

Fig. 2 Gopher: sensing node

2.2 Roccas: Data aggregator

Roccas is the wireless data aggregator of the system as shown in Fig. 3. It does not contain any sensors but has the same stackable socket of sensing node, thus sensing board of Gopher node can directly connect to the Roccas boards depending on the requirements of target SHM applications. Roccas not only aggregates the signal from multiple daisy-chained sensing nodes, frames and sends back the aggregated data to in-situ sever but it also distributes power to the sensing nodes via CAN bus. To enhance the system flexibility, it is built in many options for the aggregated data: logging data to Secure Digital (SD) card, transmitting the data over one of the wireless technologies, which may be Wi-Fi (by default), XBee pro (up to 1 km), Xstream (up to 64 km). Such multiple radio transceivers would be also configure the redundancy line against the failure of

the existing network.

The Wi-Fi module of DuraMote system supports both *infrastructure mode* and *ad-hoc mode*. In particular, ad-hoc mode is useful in configuring flexible Wi-Fi network because Ad hoc networking enables for wireless systems to connect with each other as peers as they join and leave a network over time, without requiring the support of the in-situ base station. In more detail, in order to find out nearby DuraMote to form the ad hoc network, Roocas will send out a heartbeat message to the broadcast IP address. The DuraMote system receives this heartbeat message and then responds with an ACK message. Once the DuraMote system sends out a heartbeat message to discover its neighbors, it will set the first-responding DuraMote system as its relay. It will listen to the relay for control message and send out the data record to the relay. For data communication between Roocas and Gopher, we apply to both wireless and wired interfaces. For this application of pipeline monitoring, we employ CAN (Controller Area Network) protocol for underground communication to ensure the high-data fidelity.

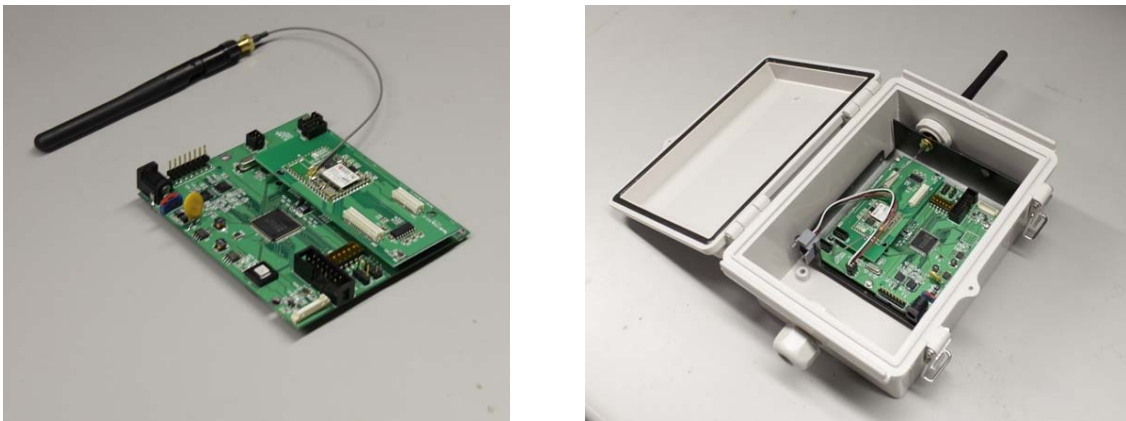


Fig. 3 Roocas: wireless data aggregator

3. Hwamyung bridge experiment

The performances of DuraMote system when used for Structural Health Monitoring of civil structures were tested on the Hwamyung Bridge (Fig. 4). The Hwamyung Bridge is a new cable stayed bridge built over the Nakdong River between the city of Busan and the town of Gimhae in South Korea. The bridge has a total length of 500 m, the main span is 270 m, and the side spans are 115 m. Two reinforced concrete towers carry the load; their top is 65 m over the deck (Fig. 5). The deck is a reinforced concrete box girder and it is supported by 72 cables. The entire structure is regular, symmetric and uniform. The bridge is a section of a multiple span bridge. The other spans are composed by a simply-supported and continuous steel-concrete deck.



Fig. 4 Hwamyung Bridge

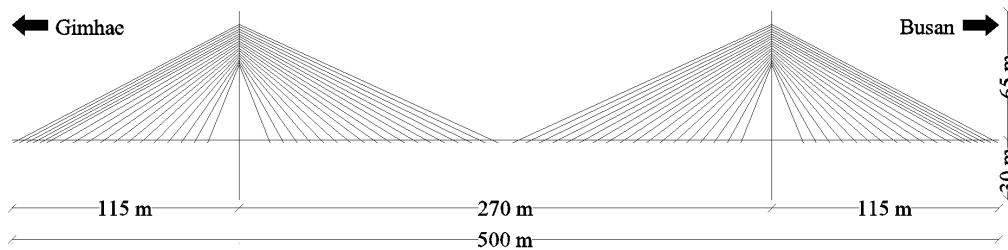


Fig. 5 Side view of the bridge

3.1 Finite element model

A Finite Element Model (FEM) of the bridge was built in Opensees McKenna(1999). The model was used to calculate the analytical natural frequencies and mode shapes of the structure for future comparison with experimental results. The model was built based on the design drawing of the bridge. Elastic beam elements were used to model the deck. The geometrical properties of each beam element are in accordance to its location because the cross-section of the deck varies within the span. Fig. 6 shows a typical cross section of the deck. To have an idea of the size of the cross-sections Fig. 7(a) shows the inside of the deck and Fig. 7(b) shows the inside of the tower.

Table 1 shows the geometrical properties of the different cross-sections, for the deck only the properties of one of the cross-sections are reported.

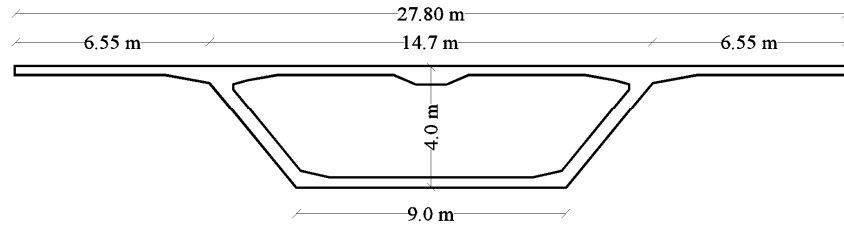


Fig. 6 Cross section of the deck of the bridge

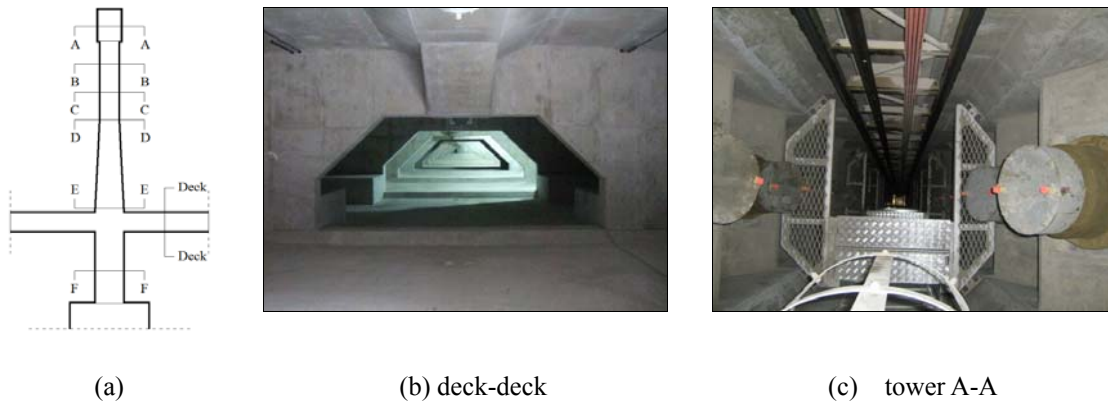


Fig. 7 Cross section of the deck of the bridge

Table 1 Cross section of the deck of the bridge

	Deck	F-F	D-E (average)	C-C	B-B	A-A
Area (m ²)	14.31	39.88	14.86	10.95	8.91	10.08
I _{XX} (m ⁴)	613.69	380.36	110.71	31.71	25.40	25.40
I _{YY} (m ⁴)	33.13	140.56	23.72	15.50	16.26	16.26
J (m ⁴)	650.00	278.26	59.47	29.29	27.89	27.89

The deck is supported by 72 cables. Each cable was designed in accordance to its locations and it has its own pretension. Six different cable types were used from the smallest 49 H, which contains 49 strands, to the largest 85 H, which contains 85 strands. All strands have the same cross-section area and are made of the same steel grade. Therefore, the geometrical and material properties of each cable, such as nominal area, tensile strength, weight, and maximum allowable force (loads + pretension), are proportional to the number of strands (Table 2). The pretension varies from 4,875 kN for the shortest cable on the side span to 9,418 kN for the longest cable, which supports the center of the main span. Although only four sensors were placed on the cables

the authors tried to cover all cable types, 4 out of 6 including the smallest and the largest cable (Table 2).

Table 2 Mechanical and geometrical properties of the cables

Anchorage Type/Node	49 H /211	55H /203	61 H	73H /204	75 H	85 H / 205
Strand No.	49	55	61	73	75	85
Nom. Area (mm ²)	7,350	8,250	9,150	10,950	11,250	12,750
Tensile Strength (kN)	13,671	15,345	17,019	20,367	20,925	23,715
Elastic Modulus (GPa)	195	195	195	195	195	195
Weight (kg/m)	67.54	76,34	84.14	101.00	103.60	118.35
Pretension (kN)	4,875	5,073		6,350		8,122

The cables were modeled with displacement based beam element “dispBeamColumn”. The properties of each element includes: normal stiffness, bending stiffness, torsional stiffness, distributed mass in accordance to the cable weight, and initial stress in accordance to the pretension of the cable. The boundary condition between the cables and the deck, the cables and the towers is a pin connection that takes into account the design geometry of the connection (Fig.8). Before choosing the “dispBeamColumn” element other elements were tested because the cables were the most complex and delicate element to be modeled.

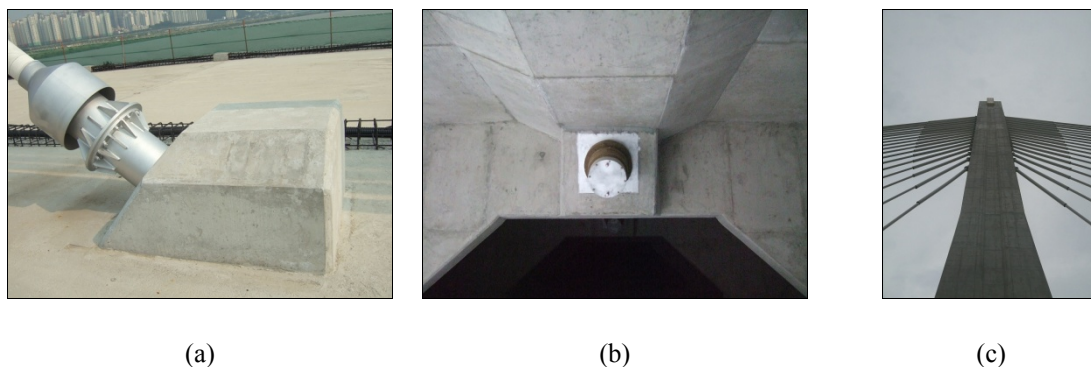


Fig. 8 Boundary conditions of the cable

Fig. 9 shows the FE model of the bridge. The boundary conditions at the bottom of the towers are a fix connection while the connection between the deck of the cable stayed bridge and the simply supported sections are a pin connection. As stated previously in this section, the bridge does not have abutments because the cable stayed bridge is only a portion of a multiple span bridge. Therefore, another valid boundary condition option could have been the combination of a roller with a longitudinal spring, which represents the stiffness of nearby spans, rather than a pin connection. However, the scope of this experiment is to assess the performances of the DuraMote

system and the modal properties of this FE model were accurate enough to compare analytical and experimental results.

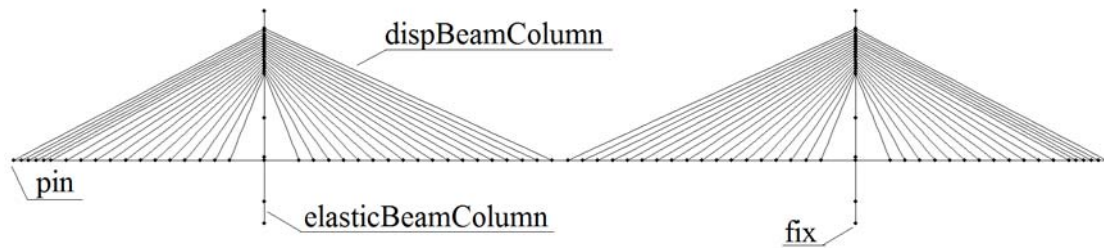


Fig. 9 Finite element model details

3.2 Sensor layout

Fig. 11 shows the layout of DuraMote system installed on the bridge. Each node includes one Rocoas, which is the data aggregation unit, and one or more Gophers, in which case Gophers are linked in series to a single Rocoas. Within the Wi-Fi network each Rocoas has its own IP address and the last three digit of the IP address will be used to name each specific Rocoas/node. The nodes from 201 through 207 were placed on the deck. These nodes include one Rocoas and one Gopher, which is equipped with two MEMS accelerometers. One sensor monitors the vertical acceleration of the deck and one sensor monitors the transverse acceleration of the deck. The nodes 209 and 210 were placed on top of the towers. These nodes include one Rocoas and one Gopher, which is equipped with three MEMS accelerometers to cover all three axes. In addition, the nodes 211, 203, 204, and 205, which are on the deck, have an additional Gopher that is placed on the nearby cable. This Gopher has only one sensor to monitor the behavior of the cable, essentially to identify its natural frequencies.

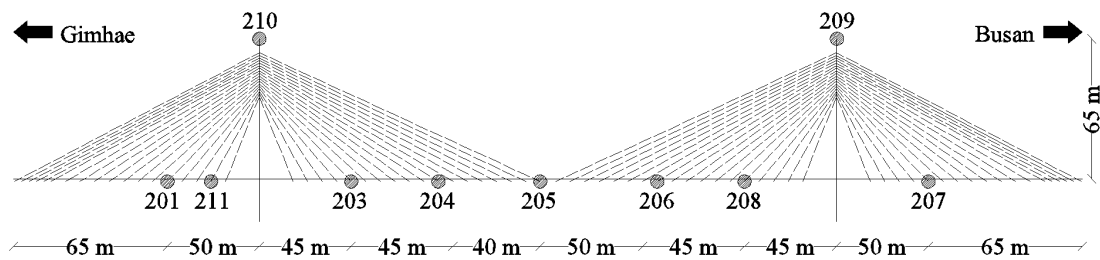


Fig. 10 Layout of DuraMote system

The entire system is compact and can be moved around with ease. Fig. 12 shows the 13 Gophers and 9 Roocas used in this experiment, plus additional units were ready to substitute a component upon its failure. The different nodes are shown in Fig. 13. Fig. 13(a) shows the node installed on the deck, Fig. 13(b) shows the node installed on the top of the towers, Fig. 13(c) shows the Gopher installed on the cable, and Figure 13d shows the server placed inside the deck near the tower on the Gimhae side.



Fig. 11 DuraMote system package

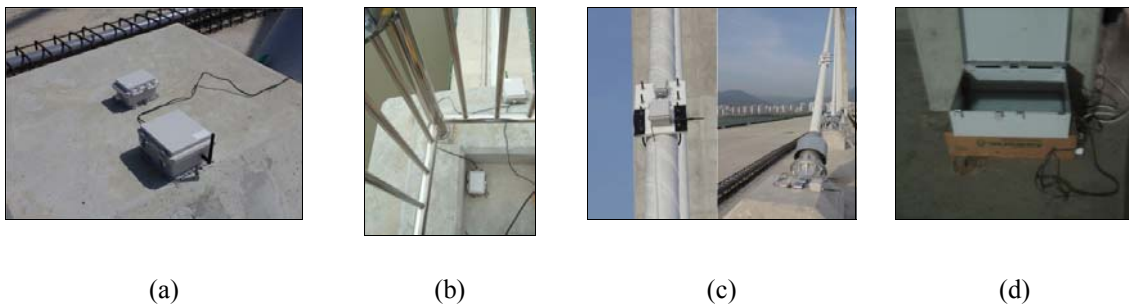


Fig. 12 Boundary conditions of the cables

Wireless sensing network is configured by nine Roocas, one base station. The data transmission between the top of the tower and the deck is connected via wireless communication despite of a distance of 65 m. The data transmission from the data aggregators on the side spans is wireless connection as well. The main span has signals which are either multi-hopped through Wi-Fi in ad-hoc mode. The base station stores all the received data and plots the results on the web page with a five second refresh rate.

3.3 Remote connection configuration

In-situ server on the Hwamyung bridge not only collects and stores the sensing data from 9ea Rocoas (i.e., 13ea Gophers) in TDMA fashion, but it also configure remote connection to report local processed data or raw data by demanding of the SCADA center in the US.

The server supports the GUI (Graphic User Interface) as a web page using time domain analysis. This web page can be remotely accessed by Wi-Fi network, Mobile network, or WiBro (Wireless Broadband) network. Fig. 14 describes the networking topology configured on Hwamyung bridge in the South Korea. As shown in the network topology, through smart phones or computers, we can see the time domain analysis results of the in-situ server, but the SCADA center is far from the bridge and located at UC, Irvine in the United States. The SCADA can require the raw data from in-situ sever whenever it is necessary to scrutinize some events to make sure on the bridge. Once the received are saved correctly from the in-situ server, SCADA can do further data processing, which may include Power Spectral Density (PSD), Singular Value Decomposition (SVD), Frequency Domain Decomposition (FDD), Short-time Fourier transform (STFT) or Contour Map. The analysis results are then rendered for display as a web page as well in the SCADA server in UC, Irvine.



Fig. 13 Remote Monitoring Topology: Smartphone or Web access through internet

4. In-situ test results

4.1 Modal parameter estimation of the bridge

In modal testing and analysis practice, one excites the structures under test by a measurable force at a reference point and collects the response data at the sensor locations. If desired, the procedure can be repeated by moving the reference point on the structure, or one may excite the structure at multiple reference points simultaneously. In this case, both the excitation and response data are available; therefore the Frequency Response Functions (FRF) can be computed. However, there are cases where the structures are subjected to natural excitations such as wind, traffic, and

wave. In this case, the excitation measurement is not available to compute the FRFs, therefore one needs to rely only on the response data. The output-only methods refer to such cases.

Frequency Domain Decomposition (FDD) by Brincker (2001) is a well-accepted modal parameter estimation technique in structural engineering applications to deal with the cases where the excitation measurement is not available. In FDD technique, the FRF is replaced by the power spectral density. FDD has two computational steps: In the first step, the cross power spectral densities between all available channels are computed, and power structural density matrix is formed. There are standard algorithms available to compute power spectral density functions, for example the Welch's algorithm (put ref). In the second step, the power spectral density matrix is factorized by the Singular Value Decomposition (SVD) at each frequency line.

FDD is based on the fact that in the vicinity of the resonance, the structural response can be approximated by a few modes. The SVD of the power spectral matrix provides the resonance of the structure, and the number of the modes that participate significantly in the response around that resonance frequency. The mode multiplicity, which might be case for symmetric structures, can also be detected by SVD. For more details the readers are referred to the paper by Brincker (2000) and Shih (1988).

The natural frequencies of the system were identified using the Frequency Domain Decomposition method (FDD) Brincker (2001). FDD is a simple but accurate method to identify the modal properties of a structure: natural frequencies, mode shapes, and damping ratio. The method is composed by two steps. In the first step, the PSD matrix of the response is calculated for each ω_i . In the second step, the PSD matrix is decomposed using SVD, Eq. (2).

$$\hat{G}_{yy}(j\omega_i) = U_i S_{+i} U_i^H \quad (2)$$

where $G_{yy}(j\omega_i)$ is the PSD matrix of the response, which is calculated from the data collected by the accelerometers, U_i holds the singular vector u_{ij} , and S_i is the diagonal matrix holding the singular value s_{ij} .

When plotted in the frequency domain the first singular value s_{ij} of each matrix S_{+i} is used to identify the natural frequencies of the structure. Each singular value represents an equivalent Single Degree Of Freedom (SDOF) system.

For example, in Fig. 17 the s_{ij} plot in the frequency domain is used to identify the natural frequency of the system for a 5 minutes signal. The natural frequencies can be identified manually or using an automated peak picking technique. Furthermore, the u_{ij} vector is used to identify the mode shape associated with the corresponding natural frequency.

Four different $G_{yy}(j\omega_i)$ PSD matrix were assembled to identify particular natural frequencies (Fig. 16). A 7x7 PSD matrix that includes the vertical accelerometers along the center line of the deck was used to identify the vertical natural frequencies and mode shapes of the deck. A 7x7 PSD matrix that includes the transverse accelerometers along the center line of the deck was used to identify the transverse natural frequencies and mode shapes of the deck. Furthermore, the accelerometers on the towers were analyzed with two different matrices. A 2x2 PSD matrix that includes the longitudinal or transverse accelerometers on the top of the towers was used to identify the natural frequencies and mode shapes of the towers. A 9x9 PSD matrix that includes the vertical accelerometers on the center line of the deck and the longitudinal accelerometers on the top of the towers was used to identify the vertical natural frequencies and mode shapes of the bridge and to

study the interaction between the towers and the deck. Finally, a 2x2 auto PSD matrix was used to identify the natural frequencies of each instrumented cable.

The MEMS analog signal is sampled at 450 Hz. The dominant natural frequencies of a cable stayed and suspension bridge are known to be far below the sampling frequency of 450 Hz. Nevertheless, a high sampling frequency of 450 Hz was used to test the robustness and efficiency of the wireless network.

$$G_{yy}(j\omega_i)$$

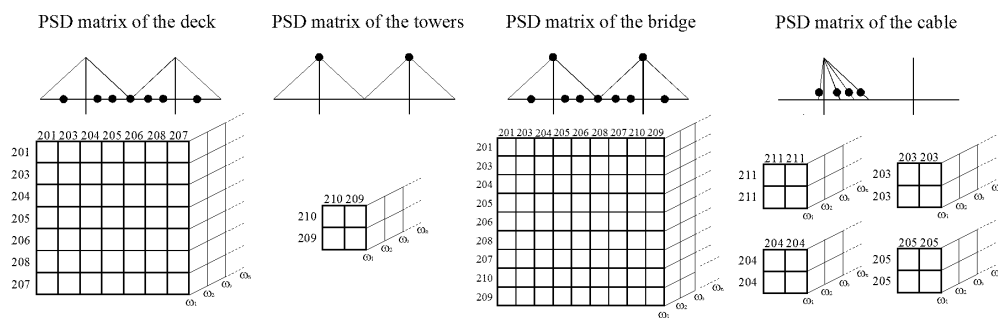


Fig. 14 The different PSD matrices

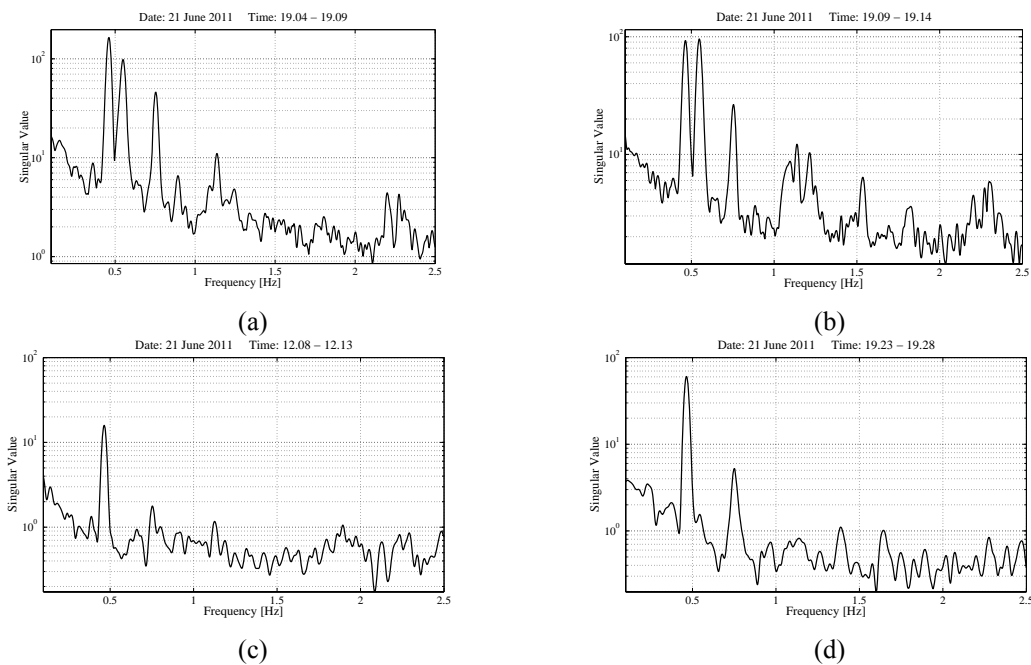


Fig. 15 samples FDD of the vertical direction

The data were stored on the server in separate files; each file contains 5 minutes record. The FDD was performed on each matrix described above for every recorded data, which is a 288 time windows of 5 minutes every day for 3 months. However, most of the time, especially during night time, there is no white noise because the bridge is still under construction and it is not open to the traffic yet. Instead, during day time trucks are operating on the bridge creating the necessary white noise to identify the natural frequencies. Samples of FDD results are shown in Figs. 17 and 18. At different times, different natural frequencies were excited but overall 0.465 Hz, 0.551 Hz, 0.643 Hz, 0.752 Hz, 1.072 Hz, 1.134 Hz, 1.276 Hz, 1.522 Hz, and 2.270 Hz were identified as vertical natural frequencies. The identification of the transverse natural frequencies was harder because peaks are smaller, and the wind doesn't excite the transverse natural frequencies often. 2.475 Hz is the most prominent natural frequencies, 0.797 Hz and 1.478 Hz could also be identified (Fig. 18). The FDD of the transverse accelerometers at the top of the towers never indicated any transverse natural frequencies for the tower.

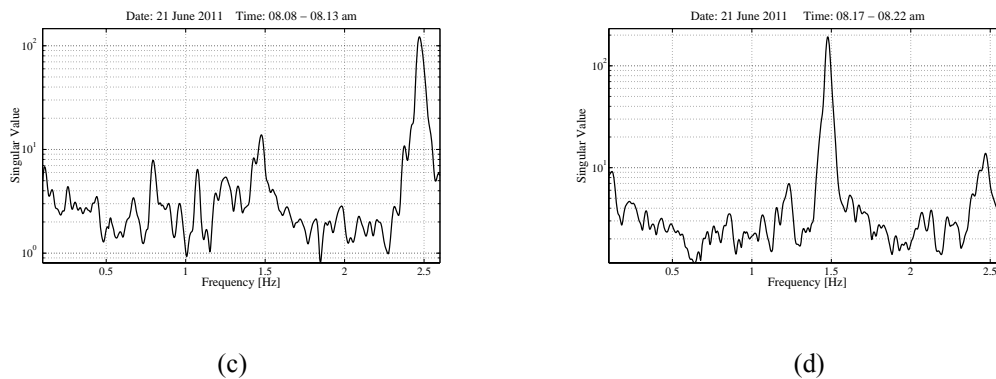


Fig. 16 samples FDD of the transverse direction

4.2 Comparison between experimental and analytical modal properties

The experimental natural frequencies, which were picked manually from the first singular value of the S_{+i} matrix, were compared with the analytical natural frequencies, which were obtained from the eigenvalue analysis of the FE model (Table 3). From the data 4 transverse and 7 vertical natural frequencies were successfully identified and they are in good agreement with the analytical results despite the fact that the FE model is based only on the design drawing and it was not calibrated on the actual data.

Two comments about Table 3 have to be stated. First, 1.072 Hz is an experimental vertical natural frequency but it is not present in the analytical model because, as stated in section 3.1 a pin connection was placed at the end of the side span rather than a roller with a calibrated longitudinal translation spring. Second, 2.475 Hz is identified as a transverse natural frequency but the eigenvalue analysis of the FE model indicates that it is the first torsional natural frequency with a transverse component. This fact could not be validated with the experimental results because the sensors were placed on the center line of the deck and they were therefore unable to track any

torsional behavior. However, this will be investigated in a future experiment.

Table 3 Identified natural frequencies

Direction	Experimental	Analytical	Difference
transversal	0.413 Hz	0.476 Hz	15.25%
vertical	0.465 Hz	0.484 Hz	4.11%
vertical	0.752 Hz	0.833 Hz	10.79%
transversal	0.797 Hz	0.782 Hz	1.88%
vertical	1.072 Hz	*	*
vertical	1.134 Hz	1.165 Hz	2.73%
vertical	1.276 Hz	1.219 Hz	4.47%
transversal	1.478 Hz	1.238 Hz	16.24%
vertical	1.522 Hz	1.561 Hz	2.56%
vertical	2.270 Hz	2.299 Hz	1.28%
transversal	2.475 Hz	2.112 Hz	14.67%

The analytical mode shapes associated with their respective natural frequency are shown in Fig. 19. The experimental mode shapes were calculated from the singular vector u_{ij} of the U_i matrix associated with the s_{ij} singular value. 7 nodes on the deck and 2 nodes on top of the towers are not enough to estimate accurate mode shapes but they are enough to associate each experimental natural frequency with the corresponding analytical natural frequency and mode shape.

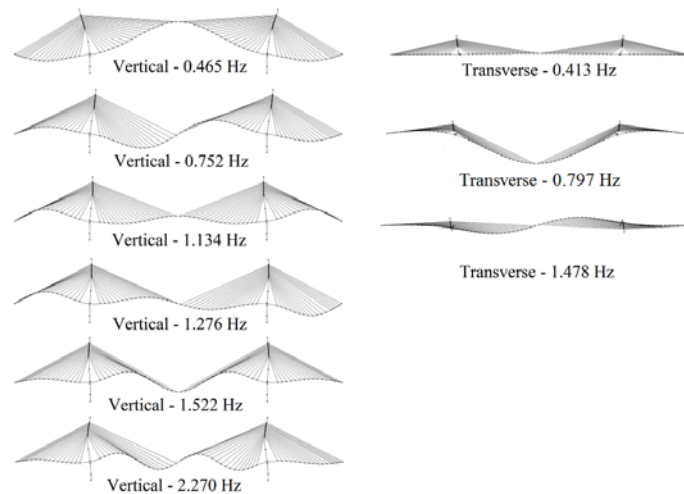
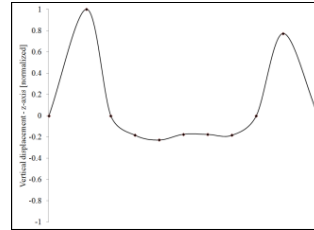
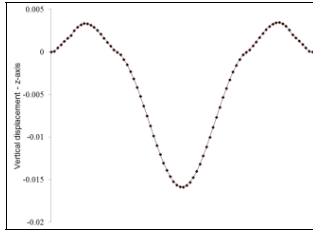
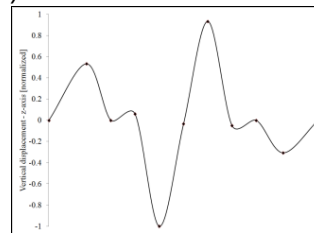
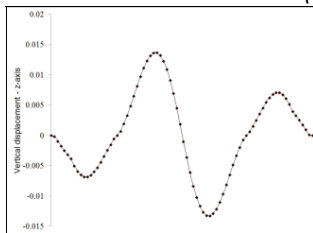


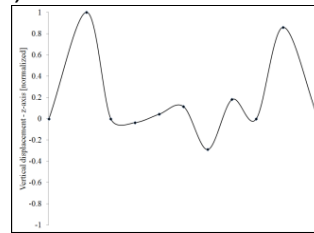
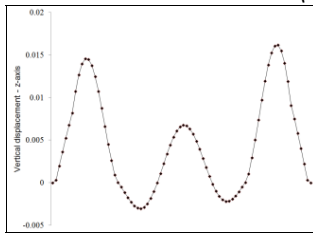
Fig. 17 mode shapes of the bridge



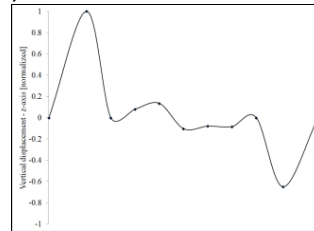
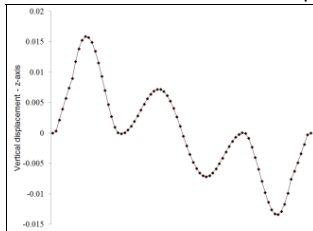
(1st mode shape 0.465 Hz)



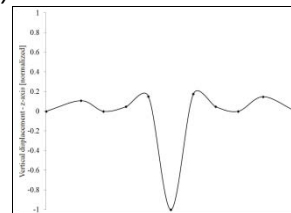
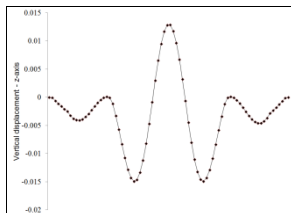
(2nd mode shape 0.752 Hz)



(4th mode shape 1.134 Hz)

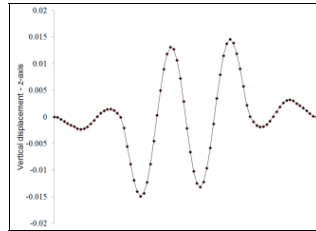


(5th mode shape 1.276 Hz)



(6th mode shape 1.522 Hz)

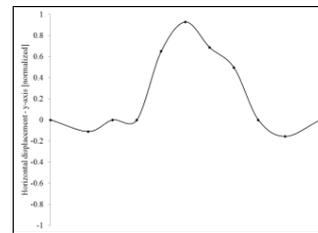
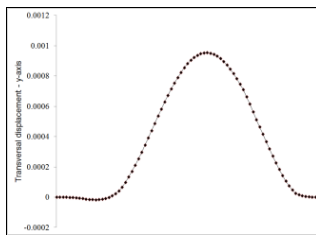
Continued



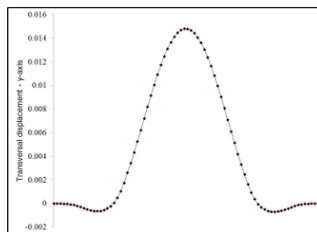
(7th mode shape 2.270 Hz “analytical”)

Fig. 18 Analytical and experimental vertical mode shapes

Fig. 20 shows the analytical vertical mode shapes of the deck and the corresponding experimental mode shape when identified. In the same way, Fig. 21 shows the transverse mode shapes of the deck. The analytical mode shapes of the deck are plotted over the nodes of the FE model, 80 points. The experimental mode shapes of the deck are plotted over the location of the sensors, 7 points. Based upon all records available the authors were able to compare: 5 vertical experimental mode shapes and 3 transverse mode shapes.



(1st mode shape 0.413 Hz)



(2nd mode shape 0.797 Hz “analytical”)

Continued

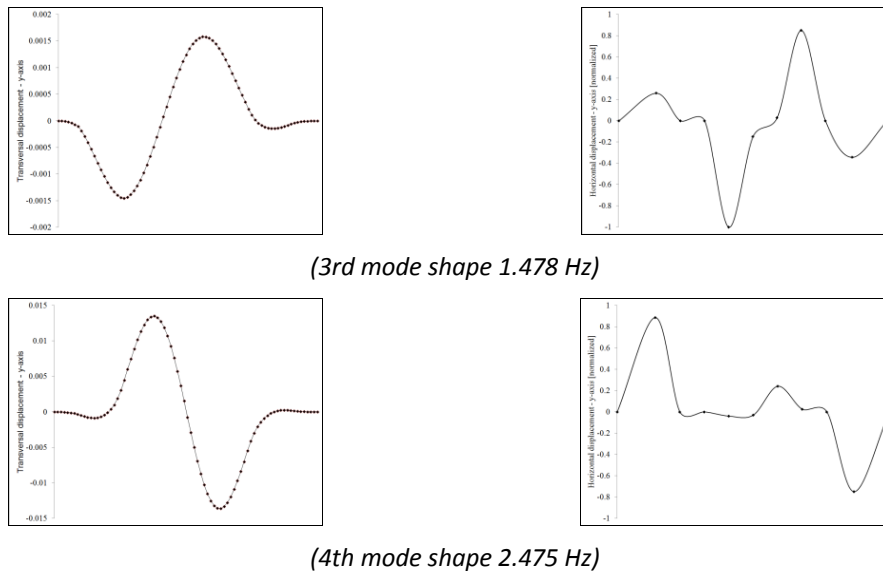


Fig. 19 Analytical and experimental transverse mode shapes

4.3 System identification of the cables

To study the modal properties of the cables 4 Gophers were placed on 4 different cables (Fig. 22). All instrumented cables are of a different type and have a different level of pretension. The authors tried to cover all types of cables, 4 out of 6 including the smallest 49H, which has 49 strands and a pretension of around 4,000 kN, and the biggest 85H, which has 85 strands and a pretension of around 9,000 kN.

Each accelerometer was analyzed separately using the FDD method. A 2x2 auto PSD matrix was calculated for each sensor and the 1st singular value s_{ij} was plotted to peak the natural frequencies. A sample plot of the first singular value s_{ij} of each cable is shown in Fig. 23. From the plot the natural frequencies can be easily identified. The mode shapes could not be extracted because only one accelerometer was placed on each cable. However, for each cable a finite element model was built using Opensees. The analytical natural frequencies match the experimental natural frequencies for each cable and the FE model indicates that the mode shapes follow the correct pattern: first harmonic, second harmonic and so on.

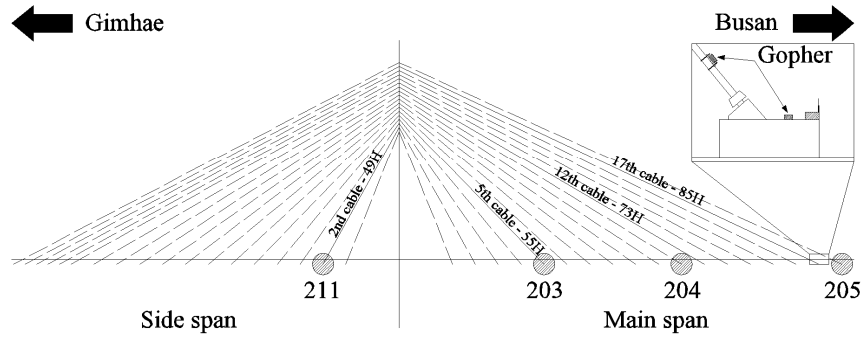


Fig. 20 layout of DuraMote system on the cables

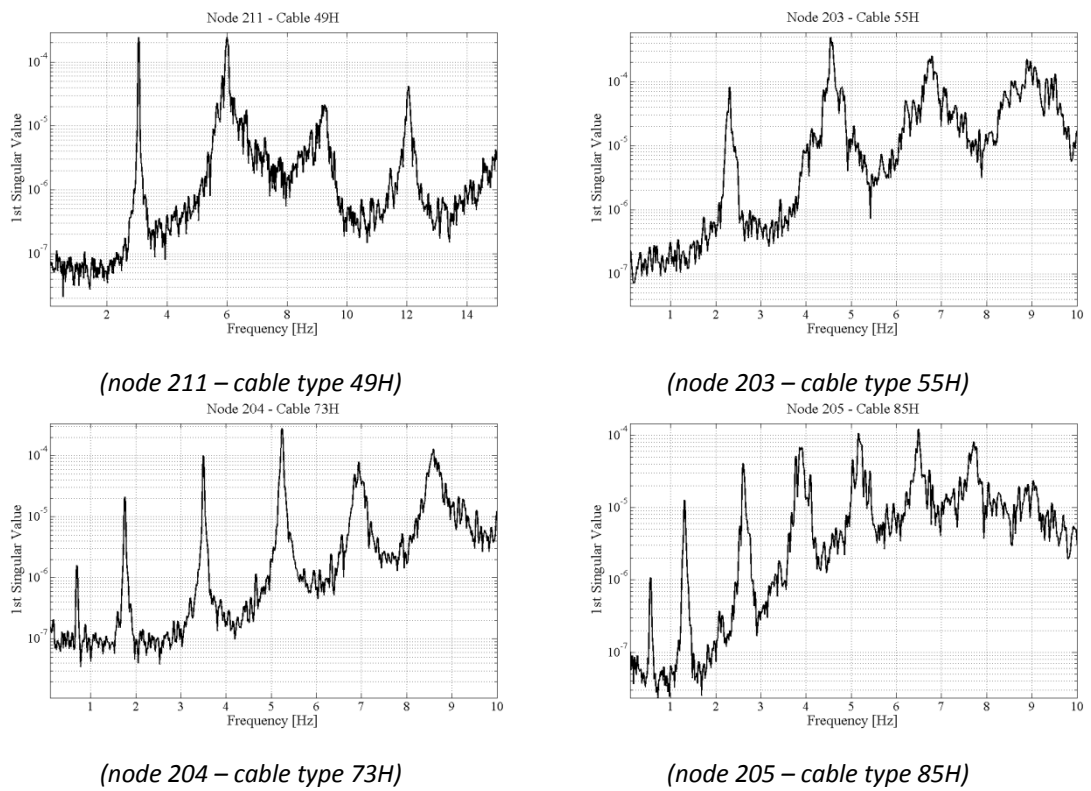


Fig. 21 samples FSD of the 4 cables

Table 4 Identified natural frequencies of the cables

Anchorage Type / Node	ω_1	ω_2	ω_3	ω_4
49 H / 211	3.054 Hz	5.999 Hz	9.261 Hz	12.05 Hz
55 H / 203	2.306 Hz	4.543 Hz	6.791 Hz	8.893 Hz
73 H / 204	1.756 Hz	3.496 Hz	5.238 Hz	6.939 Hz
85 H / 205	1.307 Hz	2.605 Hz	3.904 Hz	5.160 Hz

Table 4 reports the first 4 natural frequencies of each instrumented cable. The cut-off frequency when performing FDD of the channels on the cables was set at 20 Hz. However, the vertical natural frequencies of the deck and longitudinal natural frequencies of the tower are present in the 0-2 Hz range even inside the signals of the cables but their singular value has much lower amplitude.

These results can be compared with the natural frequency from the linear theory, Wenzel (2005). In the simplest case no bending stiffness, small cable sag and hinged support are considered. The natural frequencies are calculated from Eq. (3)

$$f_k = \frac{k}{2L} \sqrt{\frac{N}{m_L}} \quad (3)$$

where f_k is the k th natural frequency, L is the length of the cable, N is the axial force, and m_L is the mass per unit length of the cable.

The bending stiffness has to be taken into account when the ratio between the diameter of the cable and its length increases. As stated by Wenzel (2005), the influence of this ratio is remarkable for higher natural frequencies. The bending stiffness is included in the calculation of the natural frequencies of the cable using Eq. (4)

$$f_k = k\bar{f} \left(1 + \frac{2}{\xi} + \frac{1}{\xi^2} \left(4 + \frac{k^2 \pi^2}{2} \right) \right) \quad (4)$$

$$\xi = L \sqrt{\frac{N}{EJ}} \quad (5)$$

$$\bar{f} = \frac{1}{2L} \sqrt{\frac{N}{m_L}} \quad (6)$$

where ξ is the nondimensional stiffness, EJ is the bending stiffness of the cable.

The identifies experimental natural frequency, the natural frequency from Eq. (3) where the bending stiffness is not considered, and the natural frequency from Eq. (4) where the bending stiffness is indeed considered are compared in Table 5. The comparison indicates a good

agreement between the design values and the experimental values.

Table 5 Comparison between experimental and design value of cable natural frequency

Anchorage Type / Node	ω_1 Experimental	ω_1 (Eq. (3))	ω_1 (Eq. (4))
49 H / 211	3.054 Hz	3.545 Hz	3.602 Hz
55 H / 203	2.306 Hz	2.653 Hz	2.686 Hz
73 H / 204	1.756 Hz	1.592 Hz	1.604 Hz
85 H / 205	1.307 Hz	1.162 Hz	1.170 Hz

4.4 Lessons from the field experiment

The real field experiment was conducted from June 21, 2011 to August 30, 2011 on Hwamyung Bridge in Busan, South Korea to validate our system performance in terms of high-fidelity data, real-time monitoring, robustness, high wireless throughput, and local data saving. In this deployment, the utility power was available thereby continuous long term SHM by DuraMote sensing system was possible without any batteries or energy harvesters utilized in the deployment to Vincent Thomas in San Pedro, CA, USA. From Hwamyung Bridge deployment, several crucial lessons are learned in the viewpoint of harsh environmental conditions such as a heavy rain storm due to a typhoon (on June 15, 2011), a sand dust wind, and high temperature and humidity.

Considering outdoor deployment, NEMA 4+ (or IP 66) rating enclosures are adopted for our DuraMote system, which means that the enclosures are intended for outdoor use primarily to provide a degree of protection against windblown dust and rain, splashing water, and hose directed water; and to be undamaged by the formation of ice on the enclosure. However, despite of NEMA 4+ rating enclosures, water leak had occurred under severe weather condition due to a typhoon in Hwamyung bridge deployment. As a result, two sensing nodes among 13 Gophers had short-circuited, and Roocas-209 had stopped working after the typhoon was passed in that area. Furthermore, the HSDPA modem for uplink to the SCADA server in UC Irvine, CA, USA was disconnected due to the heavy rain. However, the measured data from eleven Gopher nodes were saved securely to the local data storage built in DuraMote system. As soon as the typhoon was passed, two damaged sensing nodes were replaced, and the base station on the bridge was rebooted to restore uplink HSDPA connection.

In addition, some software features were added to improve the networking capabilities. That is, the data acquisition server program was enhanced to cope with more simultaneous streaming sensing data. First, the original heart beat message has been designed as a future command channel to provide system information to the data acquisition server. Second, a faster packet-handling engine on the data acquisition server is implemented to deal with more than 10 simultaneous streams data from sensing nodes. Third, the sophisticated task manager software architecture inside Roocas is improved for a new Wi-Fi module. Furthermore, to reduce the wireless packet loss and acquire more accurate time synchronization, the firmware for both Roocas and Gopher was upgraded during Hwangyung Bridge experiment.

5. Future experiments

The future experiment of DuraMote system on the Hwamyung Bridge will have two major scopes: the detection of the torsional natural frequencies and associated mode shapes of the bridge and the evaluation of the performance of the wireless network in a confined environment, such as the reinforced concrete box girder of the bridge (Fig. 7(a)), which is similar to buried tunnels in water distribution systems. At the time of writing this paper, February 2012, DuraMote system has just been redeployed on the bridge. Six nodes are installed inside the deck (Fig. 24). Two nodes were placed on the side span and four nodes were placed on half of the main span up to the center of the bridge. Each node is composed by a single roocas, which is placed on the center line of the deck, and two gophers, which are attached to the side of the deck. Each Gophers is equipped with two MEMS accelerometers (Fig. 25).

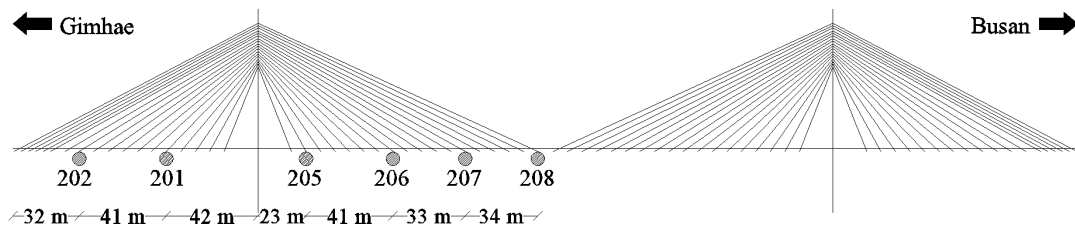


Fig. 22 layout of DuraMote system to detect the torsional mode shapes

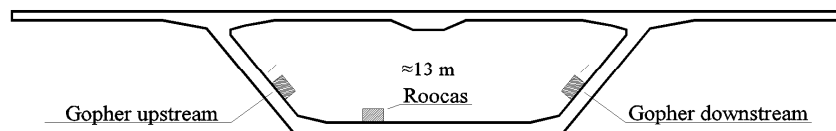


Fig. 23 layout of sensors inside the deck

This new experiment is a permanent installation of DuraMote system design to last as long as the server survives. As in the previous experiment the server is located inside the deck near the tower on the Gimhae side. However in this new experiment, the server is a dedicated desktop machine; the OS is Ubuntu 11.04 server 64bit; and the remote connection to the site is done through a 4G modem. The server on the bridge currently interacts with a server at UCI campus. The data are collected inside the server on the bridge and once a day they are compressed and sent to the server at UCI campus where they are permanently stored.

6. Conclusions

This experiment gave meaningful insight about the performance of DuraMote. It was the first large scale, remote, long term monitoring experiment and despite hardware and software problems it was successful. The system demonstrated its capabilities in monitoring the bridge which is a purpose for which it was not initially designed. The experimental modal properties of the bridge were monitored for the duration of the experiment and they are in good agreement with the analytical modal properties.

The results indicate an average packet loss of 23-25 % but it can be divided in two parts: 3-5 % packet loss in the Wi-Fi network, 20 % packet loss due to software problem, which was systematic and was fixed in the post process of the data. Additional problems were discovered in the time synchronization method but they were caused by the software that was never tested on a large scale experiment. The experimental modal properties of the bridge match the design values in both natural frequencies and mode shapes. The natural frequencies show a difference of 0.02 Hz between evening and day. A higher difference is expected between summer season and winter season but it could not be observed yet. Furthermore, the bridge is in the final construction stage with some non-structural components still missing. These components will add to the total mass of the bridge. The natural frequencies of the bridge upon completion are expected to be lower than the natural frequencies obtained in this experiment.

The Hwangyung Bridge experiment was a useful experiment. Different software and hardware problems were discovered. Fixing these problems was beneficial for the performance of DuraMote. The next large scale experiments will be on water distribution networks for the detection of pipe ruptures and leakages. The experiment will involve at least fifty Gophers and fifty Roocas. This is four times the number of Gopher used on the Hwangyung Bridge but the system will be cleared from all the problems discovered on the bridge.

6.1 Future works

In the next period DuraMote sensing network prototype will be further improved and optimized in terms of networking capabilities and power consumption. During the test some issues concerning the stability of the mote software arose which have to be addressed in order to provide reliable monitoring. The ad-hoc networking mode will be enabled to not only remove commercial wireless distribution system but also implement more flexible networking topologies. Additionally the power consumption has to be further reduced by node-level power optimization scheme, as well as minimizing the power transmission loss via CAN bus.

Acknowledgments

The authors would like to thanks Hyundai Engineering & Construction for their permission to use the bridge and their support throughout the experiment. The authors would like to thanks Mr. Ting-Chou Chien and Mr. Eunbae Yoon for their help in the deployment of DuraMote. The authors would like to thanks Prof. Jeong-Tae Kim and Prof. Shin Sung-Woo research group at Pukyung National University and Prof. Chung-Bang Yun research group at KAIST University for their help during the experiment. The authors would like to thanks Dr. Hasan Ulusoy at USGS for its insight in the system identification results.

References

- Brincker, R., Andersen, P. and Møller, N. (2000), "Indicator for separation of structural and harmonic modes in output-only modal testing", SPIE 2000.
- Brincker, R., Zhang, L.M. and Andersen, P. (2001), "Modal identification of output-only systems using frequency domain decomposition", *Smart Mater Struct.*, **10**(3), 441-445.
- Cho, S., Yun, C.B., Lynch, J.P., Zimmerman, A.T., Spencer, B. F. and Nagayama, T. (2008), "Smart wireless sensor technology for structural health monitoring of civil structures", *Int. J. Steel Struct.*, **8**(4), 267-275.
- Ghetti, A. (1980), *Idraulica*, Libreria Cortina.
- Kim, D.H. and Feng, M.Q. (2007), "Real-time structural health monitoring using a novel fiber-optic accelerometer system", *Ieee Sens J.*, **7**(3-4), 536-543.
- Kim, S., Yoon, E., Mustafà, H., Chou, P.H. and Shinozuka, M. (2011), "Smart wireless sensor system for lifeline health monitoring under a disaster event", *Nondestructive Characterization for Composite Materials, Aerospace Engineering, Civil Infrastructure, and Homeland Security IV*, San Diego, CA USA.
- Lynch, J.P., Partridge, A., Law, K.H., Kenny, T.W., Kiremidjian, A.S. and Carryer, E. (2003), "Design of piezoresistive MEMS-based accelerometer for integration with wireless sensing unit for structural monitoring", *J. Aerospace Eng.*, **16**(3), 108-114.
- McKenna, F. (1999), *Opensees*.
- Nguyen, K.D., Ho, D.D., Hong, D.S. and Kim, J.T. (2012), "Hybrid SHM of cable-anchorage system in cable-stayed bridge using smart sensor and interface", *Sensors and Smart Structures Technologies for Civil, Mechanical, and Aerospace Systems 2012*, Pts 1 and 2, 8345.
- Park, C., Chou, P.H. and Shinozuka, M. (2005), "DuraNode: wireless networked sensor for structural health monitoring", *Proceedings of the 4th IEEE International Conference on Sensors*, Irvine, CA.
- Shih, C.Y., Tsuei, Y.G., Allemang, R.J. and Brown, D.L. (1988), "Complex-mode indication function and its applications to spatial domain parameter-estimation", *Mech. Syst. Signal. Pr.*, **2**(4), 367-377.
- Shinozuka, M., Chou, P.H., Kim, S., Kim, H.R., Karmakar, D. and Fei, L. (2010), "Non-invasive acceleration-based methodology for damage detection and assessment of water distribution system", *Smart Struct. Syst.*, **6**(5-6), 545-559. *Ambient vibration monitoring*
- Wenzel, H. and Pichler, D. (2005), , Wiley.
- Yi, J.H. and Yun, C.B. (2004), "Comparative study on modal identification methods using output-only information", *Struct. Eng. Mech.*, **17**(3-4), 445-466.